EXPERIMENTAL DITCHING LOADS

H. Climent[1], G. Pastor[1], J.T. Viana[1], L. Benítez[1], A. Iafrati[2]

[1] Aeroelasticity and Structural Dynamics Department
Airbus Defence and Space. Military Transport Aircraft. Getafe (Madrid) Spain.
Hector.climent-manez@airbus.com

[2] CNR-INSEAN - Marine Technology Research Institute
Rome. Italy
alessandro.iafrati@cnr.it

Keywords: Structural dynamics. Ditching. Fluid-structure interaction.

Abstract: Ditching is a planned aircraft event that ends with controlled emergency landing in water. Four main phases may be considered in a ditching event:

— Approach: Characterized by aircraft/environment conditions before impact.

— Impact: Structural response during the impact (fluid-structure interaction).

— Landing: Subsequent motion of the aircraft until stoppage.

— Floatation: evacuation of passengers and crew.

This paper addresses some aspects of the second phase, an extreme case of fluid-structure coupling were high pressures may develop during the impact of the aircraft with water, which in turn may cause rupture of the structure, jeopardizing the required safe evacuation of crew and passengers.

At Airbus DS Military Transport Aircraft Aeroelasticity and Structural Dynamics department ditching has been a topic of continuous research for more than 12 years [1-5]. This interest is also shared by universities, research laboratories and industrial partners that have gathered together in the consortium of the European funded research project SMAES (SMart Aircraft in Emergency Situations). SMAES has devoted part of its activities to perform experimental ditching tests at the CNR-INSEAN, Rome. Data obtained from these tests can be used both, directly or indirectly to validate numerical tools / analytical theories for solving the fluid-structure behaviour during ditching.

The paper will briefly describe the tests set up and execution. The tests consist on impact of panels against water at a similar horizontal speed to the expected in a real aircraft ditching event. Panels are geometrically and structurally representative of inner fuselage skins. 64 runs were performed covering a wide variety of parameters:

— Quasi-rigid and flexible panels with different stiffness.

— Flat panels, positive and negative curvature panels.

— Metal and composite.

— Pitch angles and horizontal speeds.

Test measurements include accelerations, strains, pressures, forces and speeds.

The bulky part of the paper is focused on an elaborated analysis of the test results showing the main trends with the different parameters. Several analytical tendencies and correlations will be presented as well as the physical interpretation of these trends. Part of this information (especially time histories of pressures distributions) can be used directly in ditching analysis. In addition, all this material will be of significant help for any researcher developing numerical tools or addressing background theories that could be contrasted against these test results.

From the structural dynamics standpoint, one of the most relevant parameters is the structural flexibility: it affects the local pressures distribution and in turn strains and loads. The alleviating effect of flexibility is one of the most important outcomes of the ditching test campaign and it has critical relevance for aircraft ditching certification.

Concluding remarks highlight how these results constitute a significant step forward in the understanding of the complex fluid-structure phenomena that takes place during a ditching. The paper will end with suggestions for further work in this area.

1 INTRODUCTION

Ditching is a planned aircraft event that ends with controlled emergency landing in water. Four main phases may be considered in a ditching event:

- Approach: Characterized by aircraft/environment conditions before impact.
- Impact: Structural response during the impact (fluid-structure interaction).
- Landing: Subsequent motion of the aircraft until stoppage.
- Floatation: evacuation of passengers and crew.

This scenario is reflected in the Airworthiness Regulations that requires the aircraft manufacturer to take all necessary measures to minimize risk during ditching to allow the crew and passengers to evacuate the cabin safely.

This paper is devoted to address the dynamic loads and structural response during the second phase (i.e. the impact with water). During this phase, the high pressures derived from the impact with water of the sliding aircraft may cause rupture of the structure, which in turn may jeopardize the required safe evacuation of crew and passengers.

Ditching is an extreme case of fluid-structure interaction that constitutes a real challenge. SMAES has devoted part of its activities to perform experimental ditching tests of representative aircraft panels at full scale ditching conditions. Data obtained from these tests can be used both, directly or indirectly to validate numerical tools/analytical theories for solving the fluid-structure behaviour during ditching. The tests were performed at CNR-INSEAN, Rome, [4] and [5].

2 BRIEF LITERATURE SURVEY

A complete survey of all available literature about ditching is completely out of the scope of this paper. Nevertheless it may be convenient to mention some relevant contributions to provide with a perspective to the work presented herein.

Two classical references, [6] and [7], established the basic theory of the vertical impact of a solid surface on water. Reference [8] added some modifications to the original theory, based

in the momentum method, to estimate aircraft ditching loads. Recent studies based on these simplified theories show good agreement with experimental results, [9].

Many of the first papers focused on V shape vertical impacts as an attempt to address the hull section of seaplanes [10]. However, conventional aircrafts were designed using smooth profiles to minimize aerodynamic resistance, and therefore, there are significant differences with respect to the impact of a seaplane hull. Works [11] and [12] were devoted to rectangular flat panels and arbitrary constant cross section and [13] tested elliptical cylinders considering also horizontal speed.

Reference [14] presented the experimental investigation of the effect of the rear-fuselage shape on ditching behaviour; it is remarkable that this study is one of the first not devoted explicitly to seaplanes hulls, and its conclusions can be extended to regular aircrafts. A summary of the knowledge gained about ditching of different aircrafts in the early sixties is presented in [15]. This work identified and discussed the effects of design parameters on the ditching characteristics of airplanes based on scale-model investigations. Reference [16] is an extensive review of theoretical and experimental results applied to the seaplane impact.

Apart from these classical references, at the moment, the most extensive research is done in the fluid-structure coupling field, an example of these works may be found in [17].

3 STATEMENT OF THE PROBLEM

The final goal is to be able to simulate and predict accurately the transient loads and the aircraft structural dynamic response during a ditching event. Today this is a long term objective and to achieve it, several increasingly complex successive steps have to be completed.

The European funded SMAES project (SMart Aircraft in Emergency Situations) has been devoted to provide a wide background of high quality ditching test information that could be used for engineers to either use it directly or use it to validate their numerical simulation tools.

4 SMAES DITCHING TEST DESCRIPTION

4.1 Ditching test summary

A complete description of the test and results can be found in references [4] and [5]. A brief summary is introduced herein for completeness.

The SMAES ditching tests are set of guided impact tests of panels against water at horizontal speeds representative of aircraft skins. The objective was to measure the pressures acting on the panel and the structural deformation during the impact. To provide with a complete database, the most relevant parameters were varied during the test:

- Horizontal speed (30m/s, 40m/s, 50m/s)
- Pitch angle at impact (4°, 6°, 10°)
- Panel curvature (flat, concave, convex)
- Panel stiffness (rigid, flexible, very flexible)
- Panel material (metal –Al2024-T351–, composite)

Vertical speed:	-1.5 m/s
Total guidance structure length:	64 m
Trolley mass:	~ 600 Kg
Trolley + specimen mass:	~ 800 Kg

The trolley is accelerated by a catapult composed by a total of 8 elastic cords

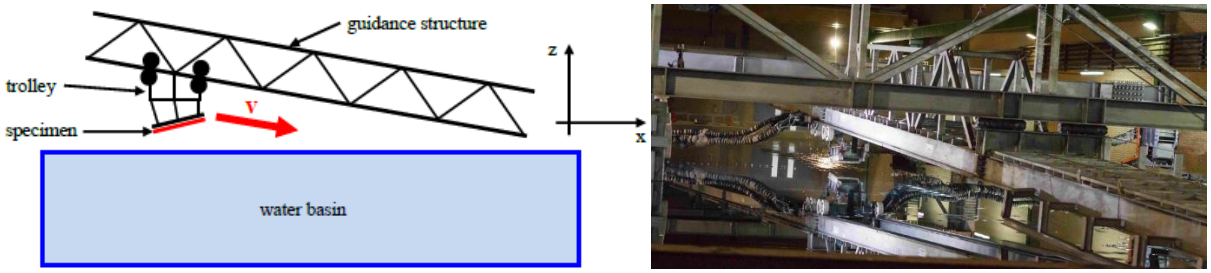

Figure 1: Schematic sketch of the guided ditching test setup

4.2 Ditching test instrumentation

The instrumentation of the guided ditching tests was very complete and differs slightly depending on the specimen and the test conditions. A typical set of instrumentation would be:

- 18 pressure transducers (18 channels)
- 6 strain gauges – two directions (12 channels)
- Velocity (1 channel)
- 2 biaxial and 2 single axis accelerometers on the panels (6 channels)
- 6 load cells to measure forces from the panel to the trolley (4 channels)

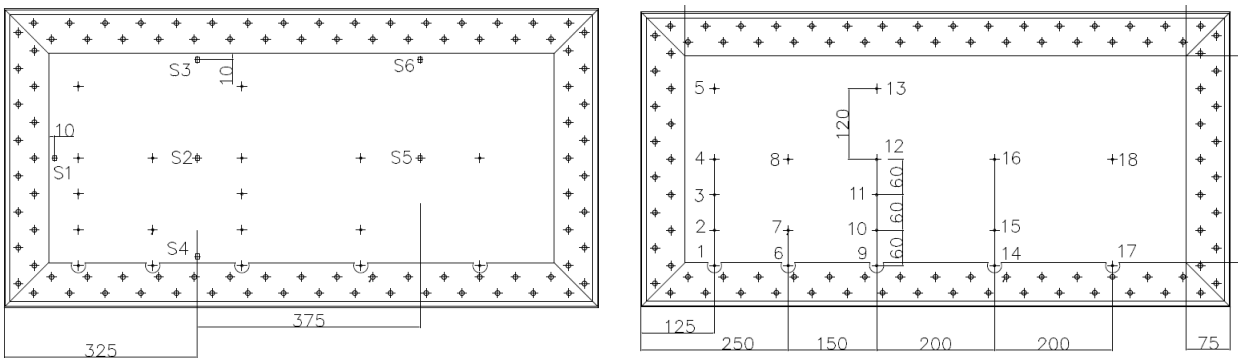

Figure 2: Positions of strain gauges (left) and pressure transducers (right)

4.3 Ditching test execution

The panel specimen, with a size of 1000 x 500 mm (typical fuselage skin panel size), was installed in a frame. The frame embedded in a trolley and the trolley guided using an auxiliary structure up to reaching the desired test conditions at the impact.

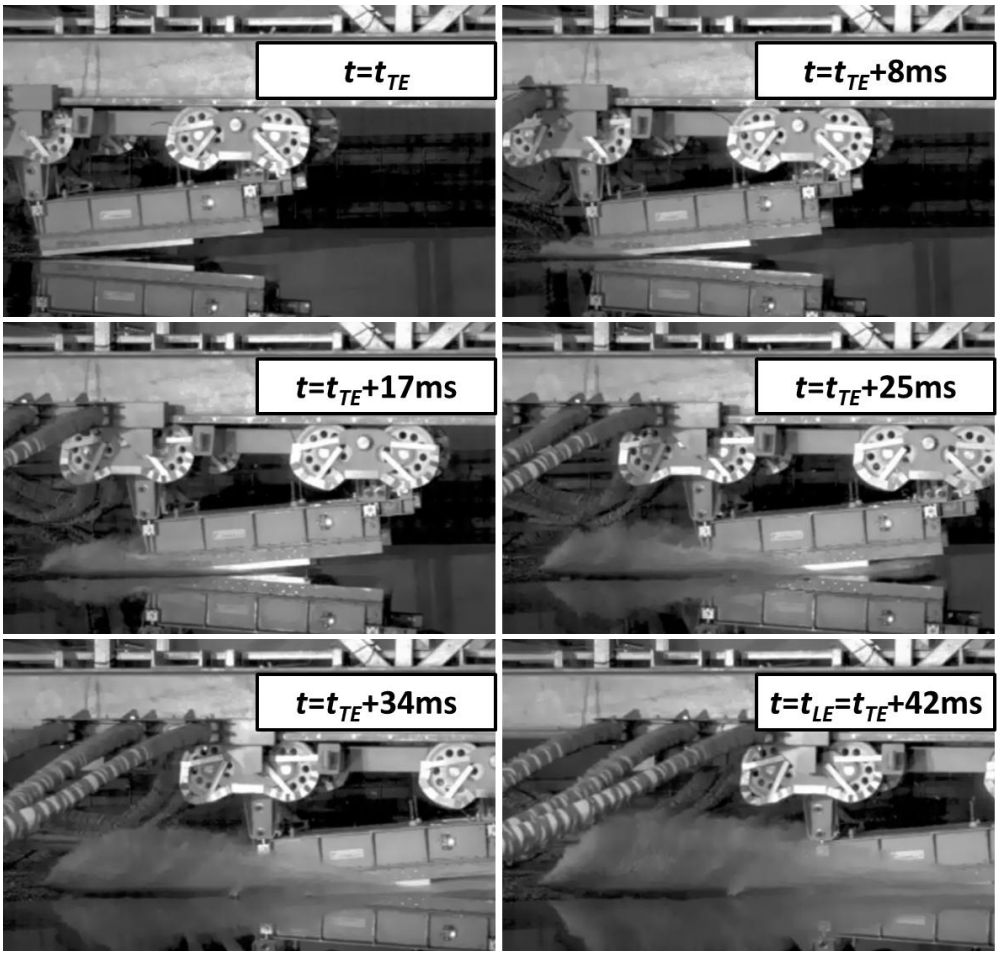

Figure 3: Pictures illustrating the guiding structure, the trolley and the specimen at impact phase

During the complete execution of each run test, six phases could be identified

1) Release
2) Acceleration: 1.00 s approximately
3) Constant velocity: 0.20 s approximately
4) Impact and natural deceleration: 0.30 s approximately
5) Forced breaking: 0.44 s approximately
6) Stop

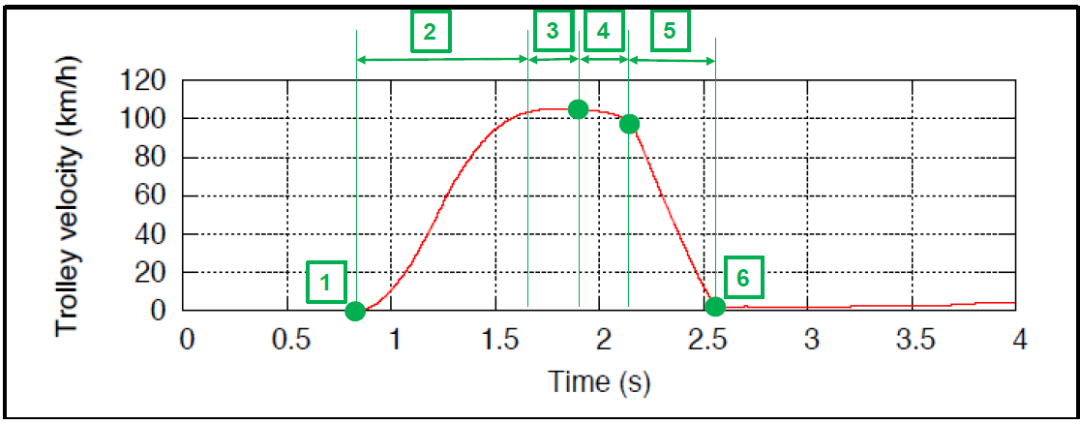

Figure 4: Phases of each ditching test run

4.4 Ditching test typical results

From the structure point of view, all the relevant phenomena occur during phase 4 in a time interval starting when the panel trailing edge gets in contact with the water surface (t_{TE}) and ending when the panel gets fully submerged (t_{LE}). The test results after t_{LE} are not considered representative of a ditching event in an aircraft, so they have not been taken into account for the analysis.

Figure 5 shows the typical behaviour of the overall forces acting over the panel and the strains produced in the transversal direction along the panel symmetry axis:

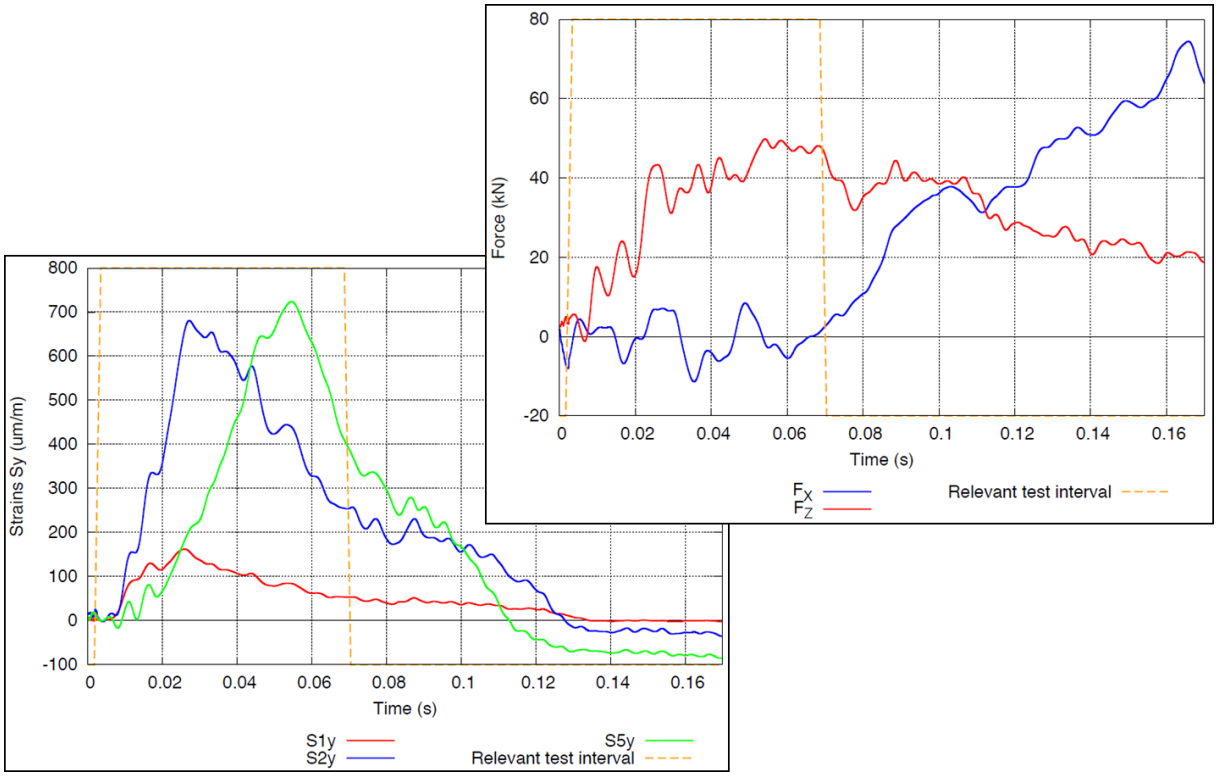

Figure 5: Typical time histories of forces and strains

Most part of the paper is devoted to present and discuss the behaviour of the pressures acting over the panel. Typical time histories for the pressures are presented in Section 5.

4.5 Test data accuracy and repeatability

As discussed in Section 4.1, a large amount of parametric variations have been performed in order to obtain a wide database with different initial conditions. To guarantee the accuracy of the test results and the independency of the environment conditions, several runs have been performed for each set of initial conditions.

A deep discussion on the accuracy and the repeatability can be found in [4] and [5].

5 TIME HISTORIES OF DITCHING PRESSURES ON FLAT RIGID PANELS

5.1 Ditching pressures. 2D Time history

Figure 6 shows the pressures time histories along the panel symmetry axis and Figure 7 along a transversal line at 0.4m from the trailing edge, for the following test conditions:

— Horizontal speed: 40 m/s

— Pitch angle: 6º

— 15 mm thick flat metal panel

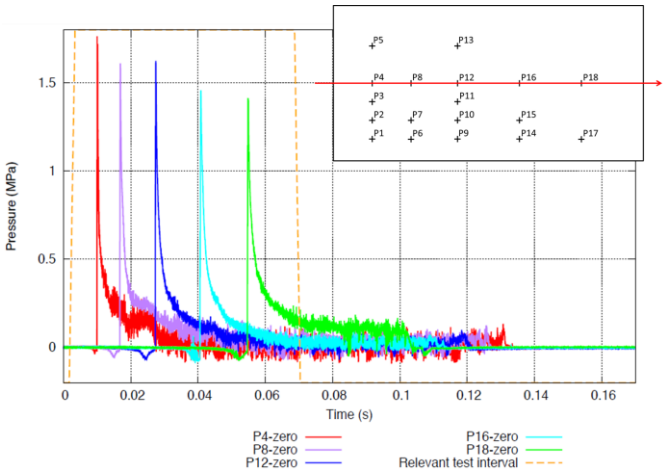

Figure 6: 2D time histories of pressures measured along panel symmetry axis

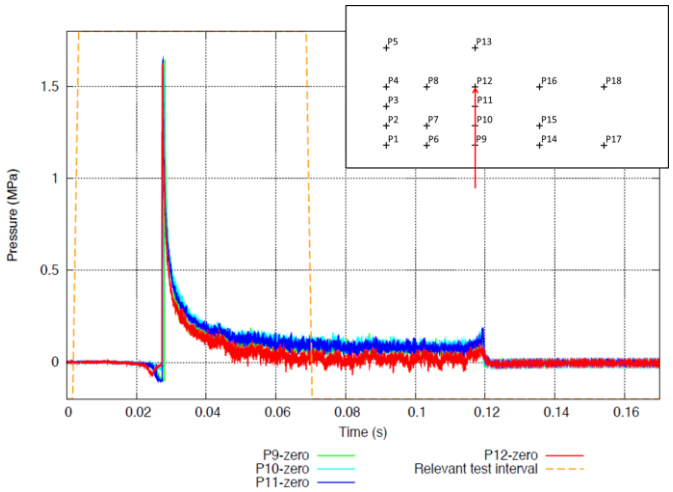

Figure 7: 2D time histories of pressures measured along a transversal line

For all the tests performed with flat quasi-rigid metal panels (15mm thick), the pressure time histories shape is always the same. They start with an abrupt peak (which is generated when the water surface gets in contact with the pressure probe), and quickly fall to a plateau which is maintained a few instants before vanishing.

There is a small time interval just before the peak in which the pressure is slightly negative. This suction is deeply discussed in [5], although considered negligible for the analysis of the pressure time histories in this paper.

For flat panels, there is no significant variation on the shape or values of the pressure signals in the transversal direction (i.e. along the lines parallel to the trailing and leading edges). There is only a very small delay due to the bending of the jet root, as discussed in [5], which will be considered negligible in this paper. Also, there must be an abrupt fall of the pressures very close to the lateral edges, where pressure must be zero to fulfil the boundary condition. Nevertheless, there is not any test information available to characterize this phenomenon because there were not sensors so close to the boundaries.

5.2 3D Time history

With the information obtained from the tests and the considerations from above, it is possible to interpolate/extrapolate the pressure signals to obtain an approximation of the pressure values among the entire panel surface.

This methodology has already been used over more complex geometries as a basis for CN-235 certification to ditching, as discussed in [1].

Figure 8 shows an example of this approximation for two time instants: with 40% of the panel surface wet and at the instant when the water reaches the flat panel leading edge. These results are quite similar to those described in [11].

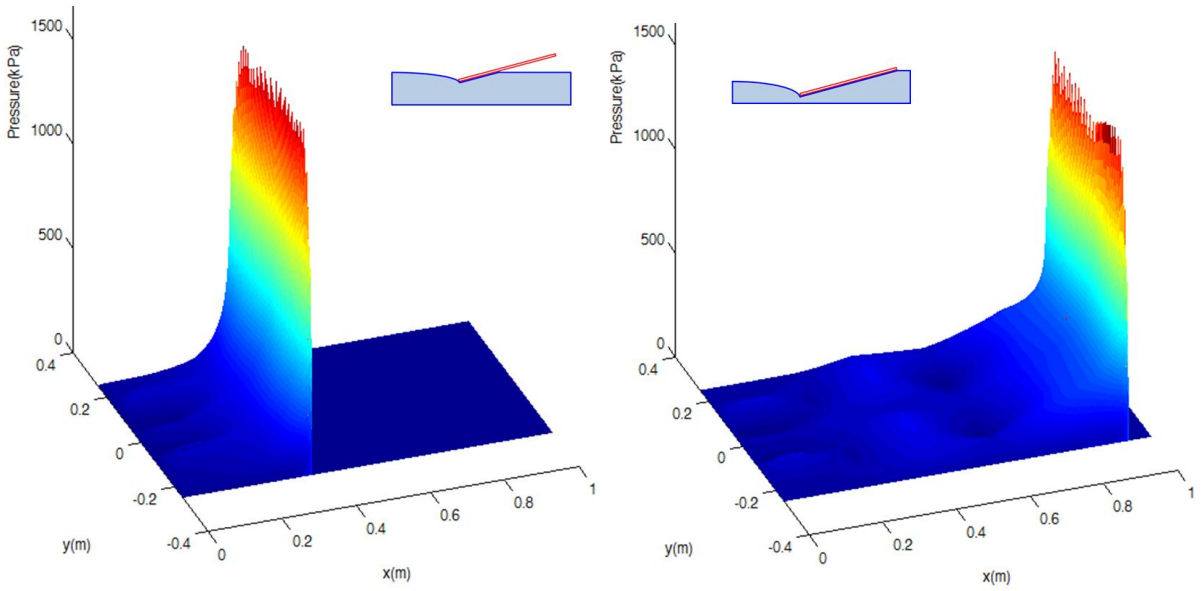

Figure 8: 3D pressure distributions with 40% panel surface wet (left) and with 100% panel surface wet (right)

5.3 Generic Ditching Pressure time history

In a general way, the pressure time history can be expressed as a function of the (x, y) position in the panel and the initial conditions described in Figure 9.

In light of the test results, the expression (1) plotted in Figure 10 seems appropriate to approximate analytically the pressure time histories obtained experimentally for a flat quasi-rigid panel ditching. As discussed in Section 5.1, the y dependency has been neglected:

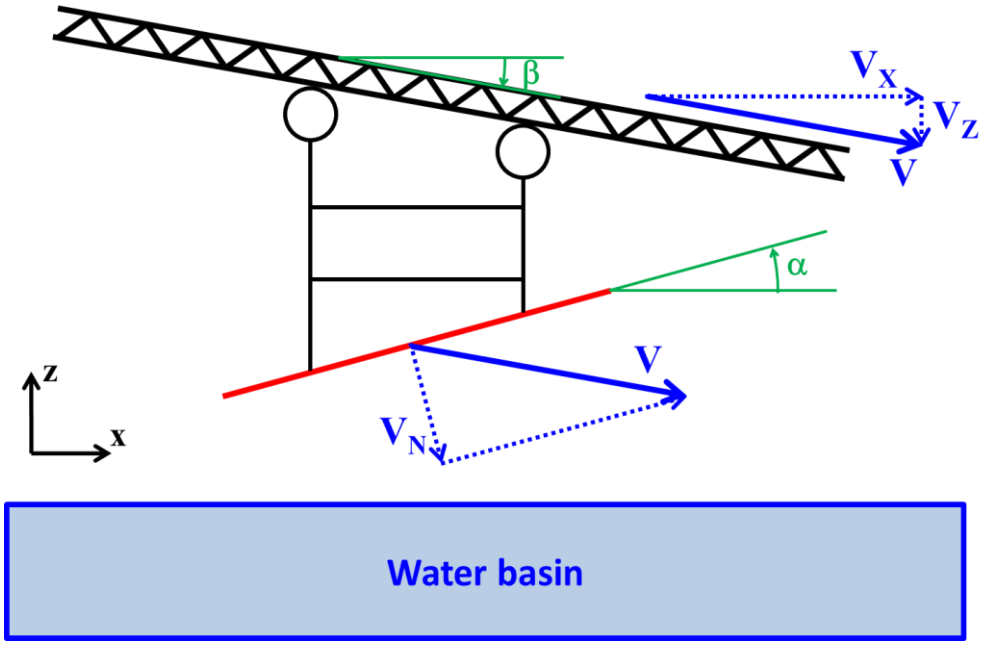

Figure 9: Initial ditching conditions sketch

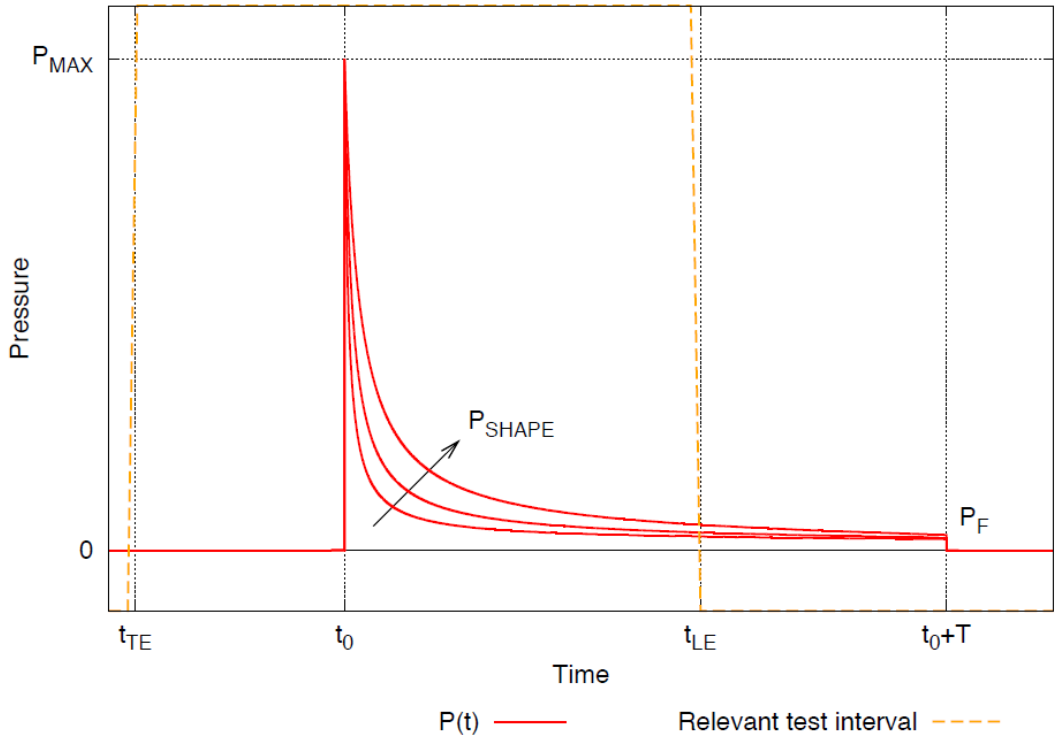

Figure 10: Analytical approximation for the pressure time histories

$$P(V_X, V_Z, \alpha, x, t) = \begin{cases} P_F + \dfrac{P_{SHAPE}}{\tan\left[\dfrac{t-t_0}{T}\dfrac{\pi}{2} + \arctan\left(\dfrac{P_{SHAPE}}{P_{MAX}-P_F}\right)\right]} & , \quad t_0 \le t \le t_0 + T \\ 0 & , \quad t < t_0 \;\&\; t > t_0 + T \end{cases} \tag{1}$$

Where:

V_X, V_Z, α	are the initial ditching conditions: horizontal speed, vertical speed and pitch angle
(x, y)	are the panel coordinates, with the origin in the central point of the trailing edge, x positive towards the direction of motion and y positive to port
t	is the time
$t_0 \equiv t_0(V_Z, \alpha, x)$	is the time instant for which $P = P_{MAX}$
$P_{MAX} \equiv P_{MAX}(V_X, V_Z, \alpha, x)$	is the peak value of the pressure time history
$P_{SHAPE} \equiv P_{SHAPE}(V_X, V_Z, \alpha, x)$	is a shape factor that determines the decay rate of the pressure time history
$P_F \equiv P_F(V_X, V_Z, \alpha, x)$	is the final pressure value at $t = T + t_0$
$T \equiv T(V_Z, \alpha)$	is an arbitrary but sufficiently large time as to make sure that the pressure time history has become almost flat

6 TEST RESULTS SENSITIVITY TO DIFFERENT PARAMETERS

The aim of this Section is to show correlations of the most relevant parameters that intervene in expression (1) with the initial ditching conditions and the position in the panel, for flat quasi-rigid panels.

6.1 Test results correlation. P_{MAX}

P_{MAX} is the peak value of the pressure time history for each pressure gauge.

Several correlating expressions have been tried with the aim to express the dependency of P_{MAX} with the initial ditching conditions parameters and with the x coordinate in a simple way.

Finally, expression (2) was found based on test results, showing a linear dependency of the peak pressure coefficient $C_{P_{MAX}}$ given by expression (3) with the difference of elevation between the pressure sensor and the trailing edge, $z - z_{TE} = x \sin\alpha$, and with the impact speed normal to the panel, V_N, given by expression (4).

$$C_{P_{MAX}} = a_M V_N + b_M x \sin\alpha + c_M \tag{2}$$

$$C_{P_{MAX}} = \frac{P_{MAX}}{\frac{1}{2}\rho V_X^2} \tag{3}$$

$$V_N = V \sin(\alpha - \beta) = \sqrt{V_X^2 + V_Z^2}\, \sin(\alpha - \beta) \tag{4}$$

$$\beta = \arctan\left(\frac{V_Z}{V_X}\right) \tag{5}$$

Where the fitting coefficients a_M , b_M and c_M are only applicable for flat quasi-rigid panels and do not depend on the initial ditching conditions. They are calculated by means of the least-squares method applied to the entire set of P_{MAX} data.

Figure 11 illustrates the dependency of $C_{P_{MAX}}$ with V_N for a selection of pressure probes:

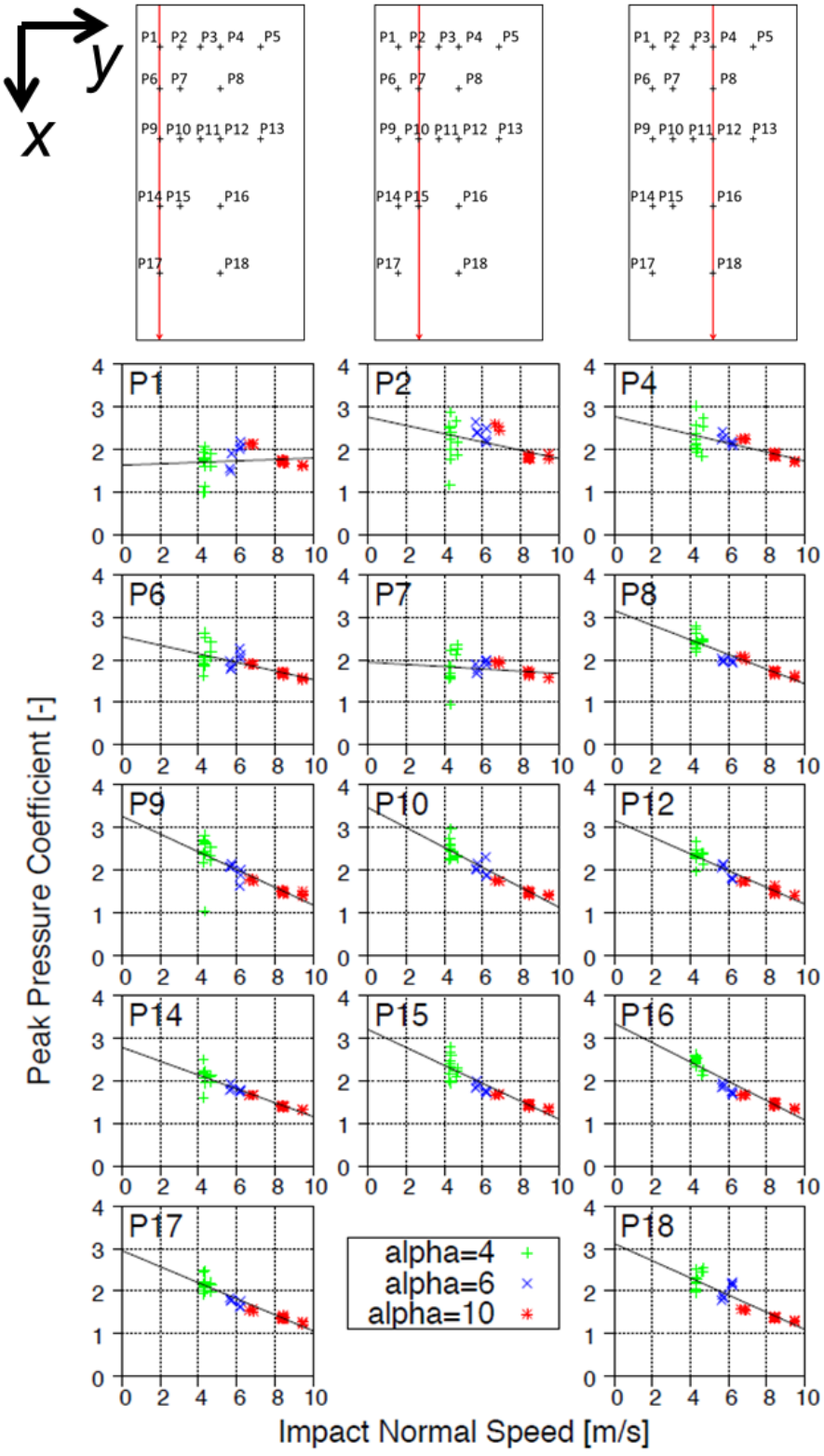

Figure 11: Sensitivity of peak pressure coefficient value to impact normal speed V_N for a selection of probes

Figure 12 shows the sensitivity of $C_{P_{MAX}}$ to $x\sin\alpha$, after the coefficient a_M has been determined:

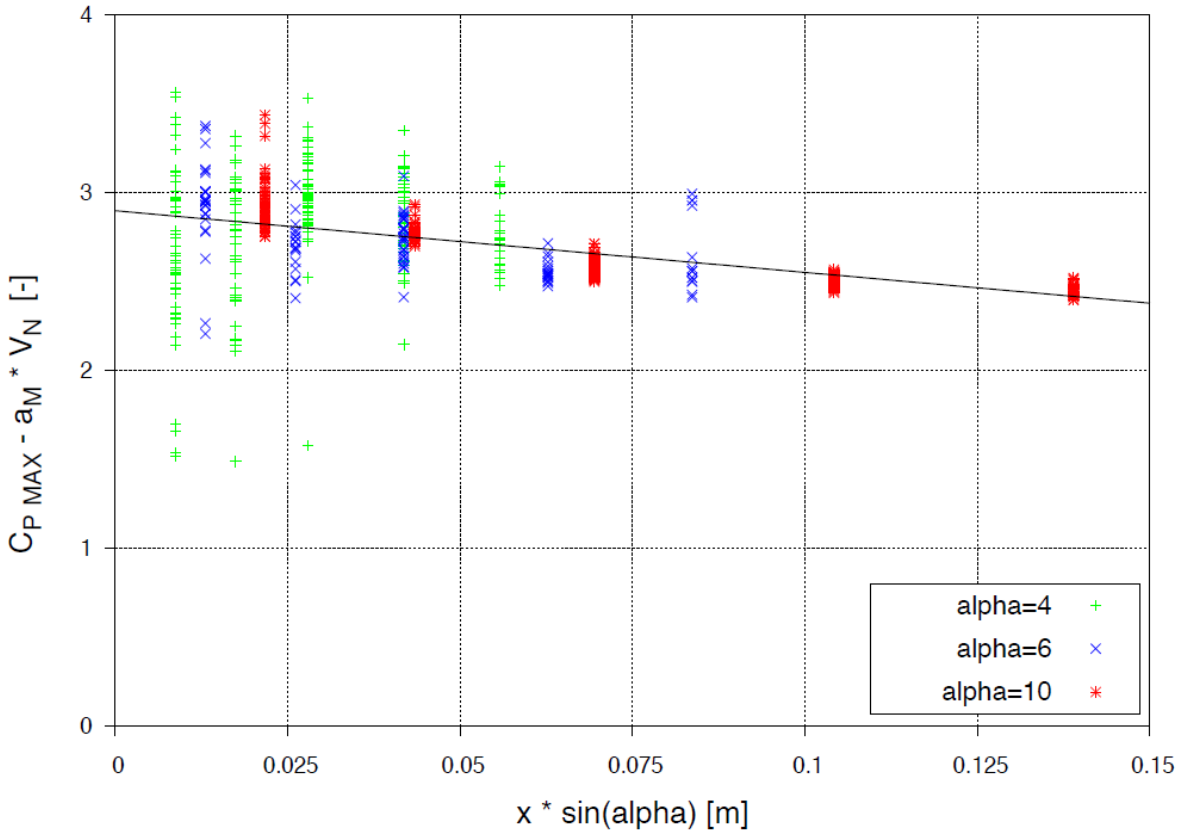

Figure 12: Sensitivity of peak pressure coefficient value $C_{P_{MAX}}$ to $x\sin\alpha$

As derived from Figure 11 and Figure 12, both a_M and b_M have negative values.

6.2 Test results correlation. t_0

t_0 is the time instant when the pressure signal starts depending on the position on the panel.

Ordinates axis in Figure 13 shows the dimensionless time elapsed between the first contact of the panel with the water surface $\tilde{t}_{TE}$ and the time instant when the pressure signal starts, $\tilde{t}_0$. Abscises axis shows the dimensionless vertical distance from the corresponding pressure probe to the trailing edge, $\tilde{z} - \tilde{z}_{TE}$. All pressure probes from all the tests with flat quasi-rigid panels are represented in this figure. Together with the test data, two slope=1 lines are represented.

$$\tilde{t}_0 - \tilde{t}_{TE} = (t_0 - t_{TE})\frac{-V_Z}{L} \tag{6}$$

$$\tilde{z} - \tilde{z}_{TE} = \tilde{x}\sin\alpha = \frac{x\sin\alpha}{L} \tag{7}$$

Where L is the panel length.

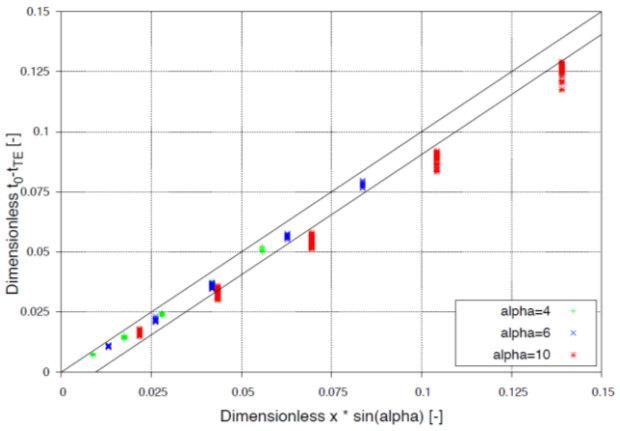

Figure 13: Sensitivity of peak pressure time instant to *x* coordinate and initial ditching conditions

Test results seem to suggest a relationship like:

$$t_0 - t_{TE} = \frac{x \sin \alpha}{-V_Z} \tag{8}$$

6.3 Test results correlation. P_{SHAPE}

P_{SHAPE} is a shape factor that determines the decay rate of the pressure time history. The Levenberg-Marquardt non-linear least squares method has been used to obtain P_F and P_{SHAPE} for each pressure time history of each flat quasi-rigid panel test. This method is applied to the smallest time interval between t_0 and t_{LE} or t_0 and $t_0 + T$, as discussed in Section 6.5.

Figure 14 shows the sensitivity of the pressure shape factor P_{SHAPE} to the x position on the panel and to the initial ditching conditions. The ordinates axis shows the dimensionless coefficient $C_{P_{SHAPE}}$ as defined in expression (9) divided by the angle of attack $(\alpha - \beta)$.

$$C_{P_{SHAPE}} = \frac{P_{SHAPE}}{\frac{1}{2}\rho V_X^2} \tag{9}$$

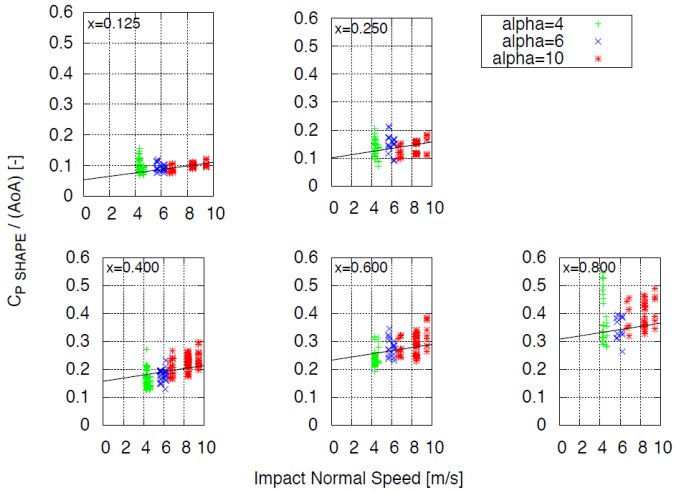

Figure 14: Sensitivity of pressure shape factor P_{SHAPE} to *x* coordinate and initial ditching conditions

A good fit of test results may be achieved using the following analytical expression:

$$\frac{C_{P_{SHAPE}}}{\alpha-\beta} = a_S V_N + b_S x\sin\alpha + c_S \tag{10}$$

Where the fitting coefficients a_S, b_S and c_S are only applicable for flat quasi-rigid panels and do not depend on the initial ditching conditions. They are calculated by means of the least-squares method applied to the entire set of P_{SHAPE} data.

6.4 Test results correlation. P_F

P_F is the pressure value at $t = T + t_0$.

P_F takes values between +13% and -10% P_{MAX}, with a mean value of 3%.

The following expression is taken as an assumption based on test results:

$$P_F = k_F P_{MAX} \tag{11}$$

Although there is a large scatter in the value of k_F, a reasonable estimation is to take the average value: $P_F = 0.03 P_{MAX}$

6.5 Test results correlation. T

T is an arbitrary but sufficiently large time to make sure that the pressure time history has become almost flat.

As shown in Figure 10, $t_0 + T$ can be set to a greater value than t_{LE}. In this case, the part of the pressure time history resulting from expression (1) between t_{LE} and $t_0 + T$ would be an extrapolation of the behaviour of the pressure as if the panel was much longer than what it really is (or as if no leading edge existed).

Despite of this, only the test data between t_0 and t_{LE} are taken into account to fit P_F and P_{SHAPE}.

On a first approximation, the simplification of taking $T = 0.1$s can be made.

If a more accurate expression is needed, the following may be used

$$T = \frac{L\sin\alpha}{-V_Z} \tag{12}$$

Where L can be arbitrarily set to 1m.

6.6 Test results interpretation

An inverse linear dependency of $C_{P_{MAX}}$ with V_N and $x\sin\alpha$ has been shown in Section 6.1. The greater the V_N and $x\sin\alpha$ values, the better the fit. Several physical phenomena may be contributing to this tendency.

The dependency with $x\sin\alpha$ and with V_N can be explained mainly by the consideration of three-dimensional effects due to the possibility for the fluid to escape to the sides of the panel, as discussed in [5]. The velocity reduction during the relevant test interval is thought to be a second order effect.

As discussed in [11], there is an initial phase on which the instantaneous speed of the peak pressure point is slightly faster than the equivalent planning velocity, i.e. the corresponding purely to the panel movement. At some point, the water flow stabilizes and these two speeds become equal. Figure 13 evidences this phenomenon, which is neglected in expression (8).

A reduction in the peak F_Z value with the pitch angle α could be expected under the aforementioned considerations. However, the parameter P_{SHAPE} shows the opposite behaviour than $C_{P_{MAX}}$ does: P_{SHAPE} increases both with $x\sin\alpha$ and with V_N. This implies that the descent rate of the pressure time histories will be lower for greater pitch angles, so that the area beneath the pressure time histories and consequently $\int P\mathrm{d}A$ will also be greater.

In light of the results obtained, the expression (1) can be used as a predictive formula in which only the initial ditching conditions V_X, V_Z, α are needed to obtain a map of the pressures actuating over the entire panel for every time instant.

Except for the curvature and flexibility effects, this formula could be used as a baseline on an aircraft ditching simulation, where the pressure time histories can extend until a time $t_0 + T$ greater than t_{LE}.

7 EFFECT OF PANEL CURVATURE ON DITCHING PRESSURES

Figure 15 shows the effect of the panel curvature radius on the peak pressure values. Black continuous lines show the mean peak pressure values for all the analysed test conditions, while green continuous lines show the mean values for all tests at 40 m/s and 4 deg pitch.

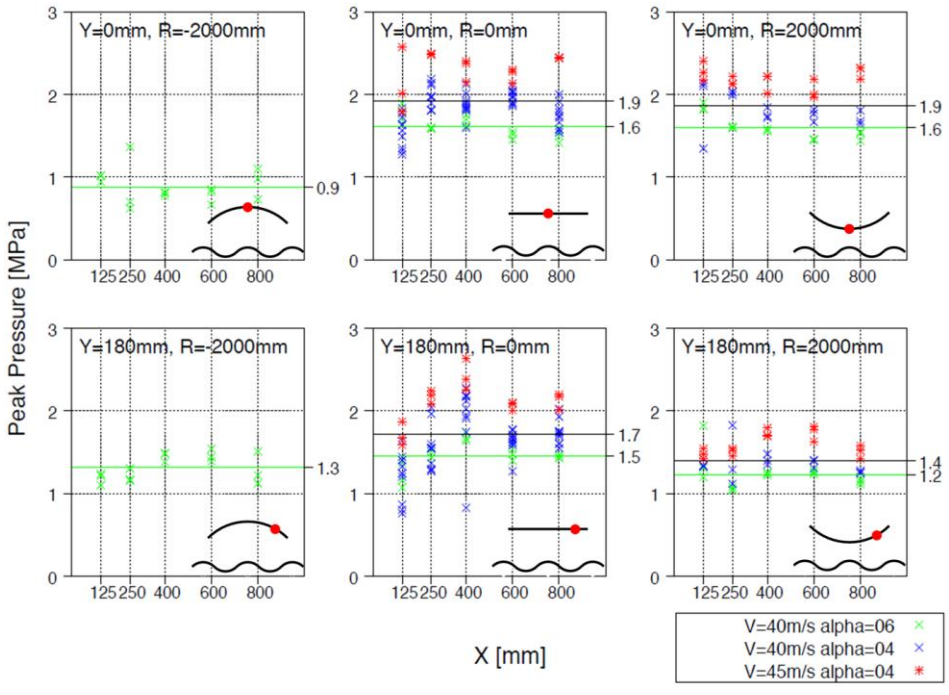

Figure 15: Sensitivity of peak pressure value to curvature

The sign convention used for the curvature radius is the following:

— First water contact is at the symmetry axis for positive curvature radius panels.

— First water contact is at the lateral edges for negative curvature radius panels.

An attenuation of the peak pressure values is observed in the most elevated zones of the cross sections of the panel: near the panel symmetry axis for the negative curvature radius and near the lateral edges for the positive curvature radius.

This behaviour seems to be related with the shape of the wave front. For non-flat specimens, pressures decay with $\left|z - z_{lowest}\right|_{x=cst}$ in a similar way as pressures decay with $x\sin\alpha$ on flat panels. Finding a good relationship with y is still a work in progress.

8 DITCHING PRESSURES ON FLEXIBLE PANELS

Figure 16 shows the sensitivity of the peak pressure values to the panel stiffness for the flexible panel cases where pressure data are available.

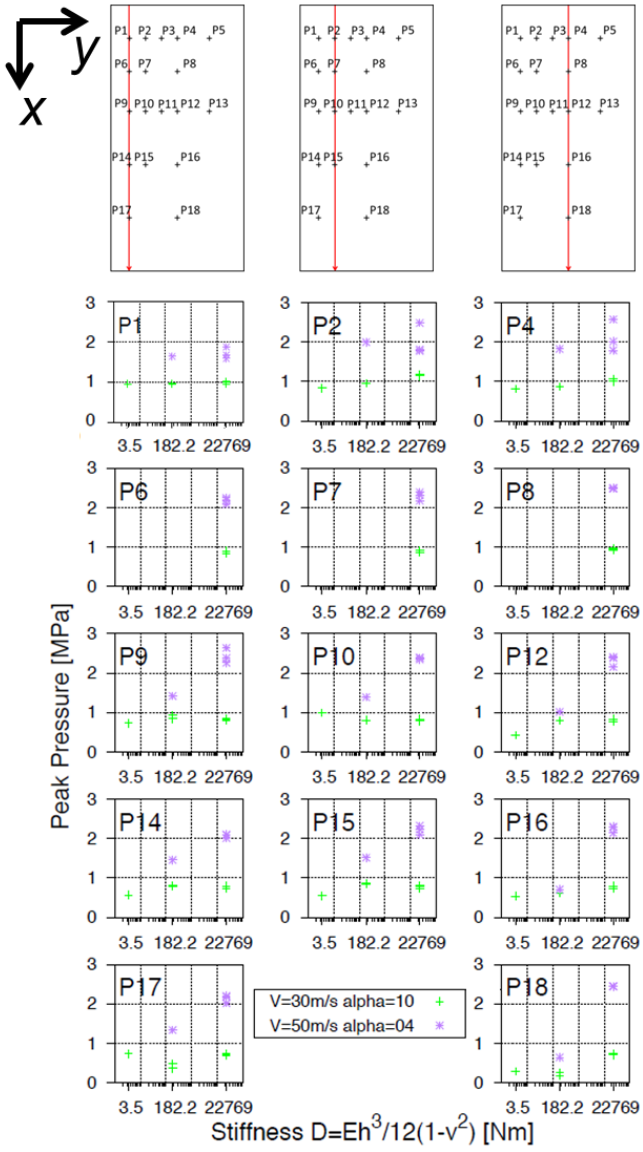

Figure 16: Sensitivity of peak pressure value to panel stiffness

Where the stiffness by surface unit is defined according to the structural flat plate theory as:

$$D = \frac{Eh^3}{12\left(1-\nu^2\right)} \tag{13}$$

Where:

E	is the material Young modulus
h	is the panel thickness
ν	is the material Poisson modulus

Figure 17 shows the same effect expressed by means of the rigid/flexible pressure ratio R:

$$R = \frac{P_{MAX}\big|_{flexible}}{P_{MAX}\big|_{rigid}} \tag{14}$$

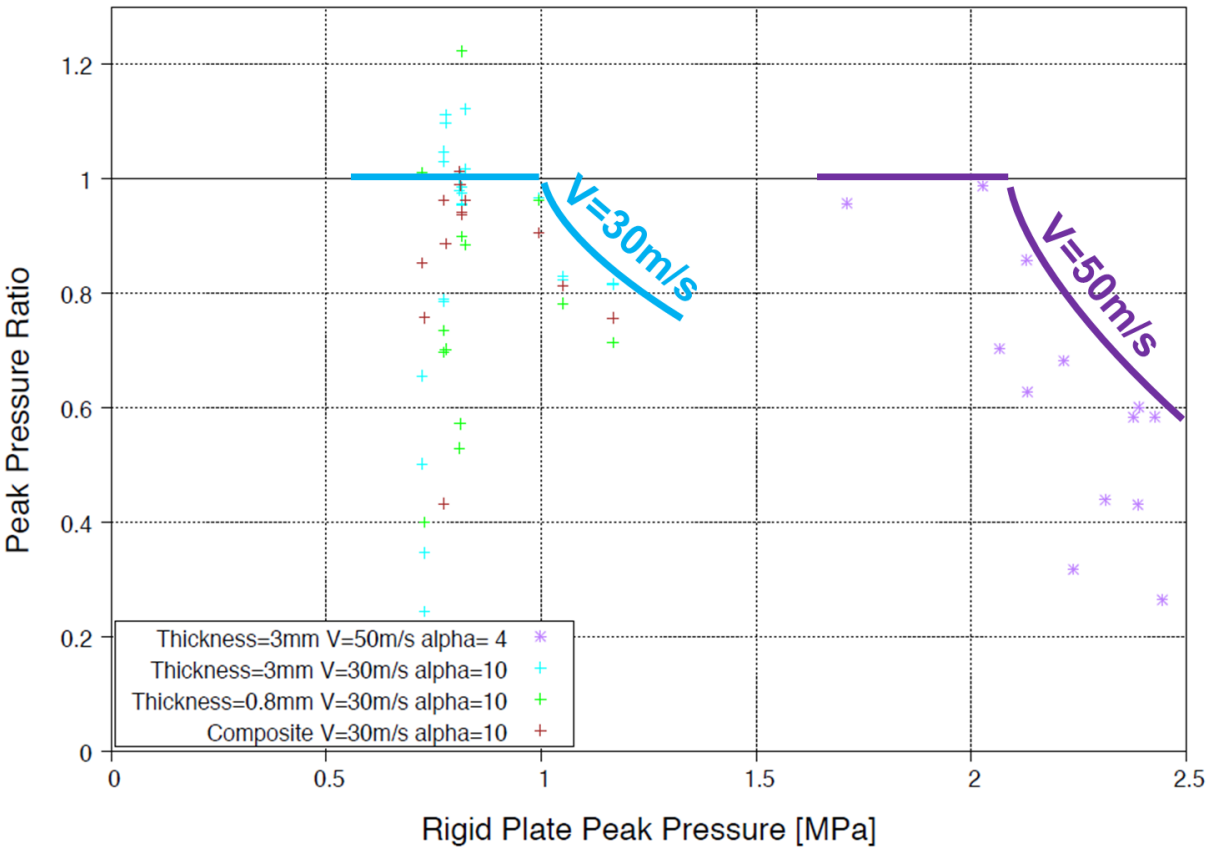

Figure 17: Deformable/Rigid peak pressure ratio

A significant decrease of the peak pressure values on flexible panels when compared with quasi-rigid panels is detected particularly for the largest peak pressures.

Finding a good relationship of ditching pressures with stiffness is still a work in progress.

9 CONCLUSIONS AND FUTURE WORK

The European funded research Project SMAES (SMart Aircraft in Emergency Situations) is a significant way forward in the understanding of the ditching phenomena. The large batch of tests performed and their high quality constitutes a solid base for researchers in coming years that will allow them to contrast analytical theories and numerical developments versus real test cases [19]. All what are considered relevant magnitudes have been measured: transient pressures, forces, accelerations, structural deformations, etc.

This paper has presented an outline of the tests performed in SMAES and some of the typical results obtained. The largest value added of the work presented herein is the digestion of some of these test results with the aim to develop design guidelines that could be used in the future to analyse a ditching scenario. In particular, the ditching pressures on flat rigid panels have been deeply analysed and the relevant trends versus the most important ditching parameters have been derived. As a result, an analytical expression that can be used for preliminary design of aircraft structures against ditching has been derived.

$$P(V_X, V_Z, \alpha, x, t) = \begin{cases} P_F + \dfrac{P_{SHAPE}}{\tan\left[\dfrac{t-t_0}{T}\dfrac{\pi}{2} + \arctan\left(\dfrac{P_{SHAPE}}{P_{MAX}-P_F}\right)\right]} & , \quad t_0 \le t \le t_0 + T \\ 0 & , \quad t < t_0 \;\&\; t > t_0 + T \end{cases} \tag{1}$$

The parameters P_{MAX}, P_F, P_{SHAPE}, t_0 and T have been determined by establishing correlations of the ditching conditions V_X, V_Z and α with test results.

The paper has continued presenting preliminary effects of both, curvature and flexibility. This part is still "work in progress" and significant effort is planned to be devoted to these two effects in the future.

- Positive curvature is the typical underbelly shape of an aircraft. Negative curvature shape is typical for an aircraft with landing gear sponsons. By considering curvature effect, the dependency with y coordinate has to be introduced. Preliminary indications suggest an alleviation of peak pressures with $\left|z - z_{lowest}\right|_{x=cst}$.
- Flexibility as another relevant effect, again because preliminary analysis tend to suggest a certain degree of pressure alleviation for large pressures.

Finally, a call for the academic world that could be interested in this research is made from these pages: it is necessary to develop analytical theories that in turn have to provide the theoretical background to support the SMAES test results. A challenging task that should be addressed sequentially in a set of increasingly complex contributions: 2D rigid; 3D rigid; 2D flexible; 3D flexible, etc.

10 REFERENCES

[1] Climent, H., Benítez, L., Rosich, F., Rueda, F. and Pentecote, N. "Aircraft Ditching Numerical Simulation," 25th Congress of International Council of the Aeronautical Sciences ICAS 2006. Hamburg, Germany, 3-8 September 2006.

[2] Siemann, M., Kohlgrueber, D., Benítez Montañés, L., and Climent, H. "Ditching Numerical Simulations: Recent Steps in Industrial Applications," Proceedings of the Aerospace Structural Impacts Dynamics International Conference, Wichita, Kansas, 6-9 November 2012.

[3] Climent, H., Viana, J.T., Benítez Montañés, L., Pérez Muñoz, J.D. and Kamoulakos, A. "Advanced Simulation (using SPH) of Bird Splitting, Ditching Loads and Fuel Sloshing," Proceedings of the ESI Global Forum 2014. Paris (France), 21-22 May 2014.

[4] Iafrati, A., Grizzi, S., Siemann, H., and Benítez Montañés, L. "Experimental analysis of the water entry of a plate at high horizontal speed." 30th Symposium on Naval Hydrodynamics. Hobart, Tasmania, Australia. 2-7 November 2014.

[5] Iafrati, A., Grizzi, S., Siemann, H., and Benítez Montañés, L. "High-speed Ditching of a Flat Plate: Experimental Data and Uncertainty Assessment." Journal of Fluids and Structures. 24 March 2015.

[6] V.Karman T. "The impact of seaplane floats during landing," NACA TN 321, 1929.

[7] Wagner H. "Uber Stoss- und Gleitvorgange an der Oberflache von Flussigkeiten. Zeitschrift fur Angewandte," Mathematik und Mechanik, 12(4), pp 193-215, 1932.

[8] Mayo W.L. "Analysis and modifications of theory for impact of seaplanes on water." NACA TR 810, 1945.

[9] Leigh B.R. "Using the momentum method to estimate aircraft ditching loads." Canadian Aeronautics and Space Journal 34, pp. 162-169, 1988.

[10] Shoemaker J.M. "Tank tests on flat and V-bottom planning surfaces." NACA TN 509, 1934.

[11] Smiley R.F. "An experimental study of water-pressure distribution during landings and planing of a heavily loaded rectangular flat-plate model." NACA TN 2453, 1951.

[12] Smiley R.F. "The application of planing characteristics to the calculations of the water-landing loads and motions of seaplanes of arbitrary constant cross section." NACA TN 2814, 1952.

[13] Schnitzer E., Hathaway M.E. "Estimation of hydrodynamics impact loads and pressure distribution on bodies approximating elliptical cylinders with special reference to water landing of helicopter." NACA TN 2889, 1953.

[14] McBride E.E. & Fisher L.J. "Experimental investigation of the effect of rear-fuselage shape on ditching behaviour." NACA TN 2929, 1953.

[15] Fisher L.J. & Hoffman E.L. “Ditching investigations of dynamics models and effects of design parameters on ditching characteristics.” NACA Report 1347, 1957.

[16] Arlotte T., Brown P.W. & Crewe P.R. “Seaplane impact. A review of theoretical and experimental results.” Ministry of Aviation. Aeronautical Research Council. Reports & Memoranda No. 3285, 1962.

[17] Shigunov V. “Berechnung der Flugzeugbewegung beim Notwassern.” Thecnische Universitat Hamburg-Harburg Arbeitsbereiche Schiffbau, Bericht Nr. 608, September 2000.

[18] Benítez Montañés, L. and Climent, H. “SMAES 36 Months Review: Guided Ditching Test and Simulations”. Airbus DS Report ME-T-NT-140004. 22-Jan-2014.

[19] Viana, J.T., Romera, J., Pastor, G., Benítez, L, Climent, H. and Siemann, M. “Numerical Simulation of Ditching Dynamic Loads” to be presented at the International Forum of aeroelasticity and Structural Dynamics, IFASD 2015, S.Petersburg, RU, 28-Jun, 2-Jul 2015.

11 ACKNOWLEDGEMENTS

Part of the work leading to the results presented has received funding from the European Commission’s Seventh Framework Programme under grant agreement no FP7- 266172 and was performed within the project SMAES — SMart Aircraft in Emergency Situations.

12 COPYRIGHT STATEMENT